第 31 卷第 5 期
2015 年 5 月

无 机 化 学 学 报
CHINESE JOURNAL OF INORGANIC CHEMISTRY

Vol.31 No.5
1003-1009

基于前驱体 Pb(OH)I 溶液法制备 $FAPbI_3$ 太阳能电池

朱慧敏[1] 王 栋[2] 于 勇[1] 段咏欣*,[1] 逄淑平*,[2] 崔光磊[2]
([1]青岛科技大学高分子学院橡塑材料与工程教育部重点实验室,青岛 266042)
([2]中国科学院青岛生物能源与过程研究所,青岛 266101)

摘要:甲脒铅碘因具有高热稳定性和较窄的禁带宽度而受到广泛关注。本工作使用羟基碘化铅代替传统碘化铅、氯化铅,通过一步溶液法制备介孔甲脒铅碘钙钛矿太阳能电池,研究退火温度对材料的结晶性、覆盖层形貌和器件的效率等方面的影响。较之传统的溶液法工艺,基于羟基碘化铅制备的甲脒铅碘薄膜表现出更为优异的热稳定性能。最终在 AM 1.5 G 一个太阳光照明下,得到了 5.8%的光电转化效率,其中短路电流为 18.6 mA·cm^{-2},开路电压为 0.67 V,填充因子为 0.47。

关键词:Pb(OH)I; $FAPbI_3$; 钙钛矿; 一步旋涂工艺
中图分类号:O611.6 **文献标识码**:A **文章编号**:1001-4861(2015)05-1003-07
DOI:10.11862/CJIC.2015.126

Solution Processed Hybrid Formamidine Lead Iodine Solar Cells Based on Pb(OH)I Precursor

ZHU Hui-Min[1] WANG Dong[2] YU Yong[1] DUAN Yong-Xin*,[1] PANG Shu-Ping*,[2] CUI Guang-Lei[2]
([1]*Key Laboratory of Rubber and Plastics Ministry of Education, Institute of polymer, Qingdao University of Science and Technology, Qingdao, Shandong* 266042, *China*)
([2]*Qingdao Key Lab of Solar Energy Utilization and Energy Storage Technology, Qingdao Institute of Bioprocess Technology, Chinese Academy of Sciences, Qingdao, Shandong* 266101, *China*)

Abstract: Formamidine lead iodine becomes extremely promising for its highly thermal stability and narrow band gap. In this work, we have employed a hydroxyl iodine lead precursor to replace lead chloride and lead iodide to fabricate a pure phase formamidine lead iodine perovskite in mesoscopic solar cells based on the one-step solution processing method and then studied the effect of annealing temperature on the material crystallinity, the morphology of capping layer and devices efficiency etc. Compared with the traditional solution processing methods, the hydroxyl iodine lead derived formamidine lead iodine film delivers an improved textured structure and thermal stability. As a result, a short circuit photocurrent density of 18.6 mA·cm^{-2}, an open circuit voltage of 0.67 mV, fill factor of 0.47, and a power conversion efficiency of 5.8% are achieved under the simulated AM 1.5G one sun illumination.

Key words: Pb(OH)I; $FAPbI_3$; perovskite; one-step spin-coating

0 Introduction

Due to the energy depletion and environmental pollution problems produced by the using of the traditional fossil energy, the development of renewable energy is attracting more and more attention [1].

收稿日期:2014-11-13。收修改稿日期:2015-03-01。
国家自然科学基金(No.51202266),青岛研究项目(No.13-1-4-228-jch)资助。
*通讯联系人。E-mail:pangsp@qibebt.ac.cn

Photovoltaic (PV) solar energy conversion has the potential to play a major role in future electricity generation[2]. Perovskite has become a hot topic in recent years and perovskite solar cells gradually move towards practical applications[3-5]. Methylamine lead halide ($MAPbX_3$) is the focus of research in perovskite solar cells for its high efficiency and the relatively easy processing[6-8]. The band gap of $MAPbI_3$ based perovskites is ~1.55 eV and there is still a large amount of light loss in near infrared wavelengths of the solar spectrum[9]. Teck Ming Koh et al.[10] reported a Formamidinium (FA) lead triiodide ($FAPbI_3$) perovskite, where a relatively larger organic FA cation ($NH_2CH=NH_2^+$) could replace the MA cation ($CH_3NH_3^+$) in perovskite structure and could result in a smaller band-gap and a power conversion efficiency (PCE) (4%). The measured band gap of $FAPbI_3$ film is ~0.07 V smaller than that of the traditional $MAPbI_3$ [11]. The improved absorption render this $FAPbI_3$ perovskite extremely attractive for next generation high-efficiency low-cost solar cells[12].

We have studied the synthesis, crystal structure and optical properties of the $FAPbI_3$ perovskite[12-13]. However, due to the large size of the organic FA cation, the synthesis of the FA containing perovskite is much more difficult than the MA containing perovskite. Generally, solution processing method requires a relatively higher annealing temperature and also can cause several side reactions, such as the sublimation of FAI and the decomposition of $FAPbI_3$, especially when the solution crystallization process is constrained within the pores of the porous titanium dioxide (TiO_2).

For the traditional lead iodide (PbI_2) based method, it is difficult to get a pure phase $FAPbI_3$ by using the PbI_2: FAI molar ratio of 1∶1. We found that increasing of the organic FAI content in the precursor solution could efficiently enhance the purity of $FAPbI_3$ perovskite and finally a power conversion efficiency (PCE) of 3.7% was obtained[12]. With the same idea, the lead chloride ($PbCl_2$) based method with the mole ratio of $PbCl_2$ to FAI of 1∶3 was used to synthesis formamidine lead iodine chloride ($FAPbI_{3-x}Cl_x$) perovsktite and a PCE of 7.5% was achieved[13]. However, the results show that the $FAPbI_{3-x}Cl_x$ perovskite capping layer coverage decreases with increasing heat-treatment temperature due to its poor thermal stability.

In this paper, we further developed an alternative method to synthesize a pure phase $FAPbI_3$ perovskite in the porous TiO_2 layer by using a lead hydroxyl iodine lead precursor Pb(OH)I. Based on such method, the effect of the annealing temperature on the crystallization, film morphology, UV absorption and devices performance were elucidated. The modified molar ratio of Pb(OH)I to FAI is 1∶3 and a PCE of 5.8% under the simulated AM 1.5G one sun illumination was achieved. Considering its textured structure, high temperature stability and the improved capping layer morphology, the efficiency of the Pb(OH)I derived $FAPbI_3$ solar cells could be further improved by modifying the processing parameters.

1 Experimental

1.1 Synthetic of Pb(OH)I

The Pb(OH)I powder was synthesized following the procedure reported by Zhu et al[14]. Analytical pure lead acetate ($Pb(CH_3CO_2)_2$) (Sinopharm Chemical Reagent Co. Ltd., China) and potassium iodide (KI) (Sinopharm Chemical Reagent Co. Ltd., China) were used as received. In a typical synthesis, 2.859 g of $Pb(CH_3CO_2)_2$ was dissolved in 30 mL distilled water (solution A), 1.258 g KI was dissolved in 15 mL distilled water (solution B). Subsequently, solution B was slowly dropped into solution A under vigorous stirring, and a faint yellow precipitate was formed. The precipitate was then separated with a centrifugal machine and collected by rotary drying at 60 ℃. The faint yellow solid was finally dried at 60 ℃ under vacuum for 2 h.

1.2 Synthesis of FAI

FAI was prepared by directly mixing 3.0 g of formamidine acetate (99%, Aladdin Chemical Co. Ltd., China) and 8.2 g of HI (45wt% in water, Sinopharm Chemical Reagent Co. Ltd., China) at 0 ℃ for 2 h. The precipitate was collected by rotary drying

at 65 ℃ for 30 min, which was followed by washing with a mixture of ethanol and diethyl ether by air pump filtration. The white solid was finally dried at 60 ℃ under vacuum for 2 d.

1.3 Synthesis of $FAPbI_3$

The precursor Pb(OH)I was firstly synthesized by reacting $Pb(CH_3CO_2)_2$) with KI (reaction **1**), $FAPbI_3$ was prepared by reacting Pb(OH)I with FAI (1∶3 in molar ratio) in DMF solution (reaction **3**) where FAI was synthesized by reacting $NH_2CH{=}NHCOOCH_3$ with HI(reaction **2**).

$$Pb(CH_3CO_2)_2+KI \rightarrow Pb(OH)I+CH_3COOK+CH_3COOH \quad (\mathbf{1})$$

$$NH_2CH{=}NHCOOCH_3+HI \rightarrow NH_2CH=NH_2I+CH_3COOH \quad (\mathbf{2})$$

$$Pb(OH)I+3NH_2CH{=}NH_2 \rightarrow NH_2CH{=}NH_2PbI_3+NH_2CH{=}NH_2I+H_2O \quad (\mathbf{3})$$

It is worth noting that the synthesized Pb(OH)I is apt to decompose under a long time or a strong light irradiation, thus it should be kept in dark before mixing with FAI.

1.4 Device Fabrication

Prior to the device fabrication, the FTO(Fluorine-doped Tin Oxide)/glass substrates were patterned by etching with Zn powder and 2 $mol\cdot L^{-1}$ HCl in distilled water. The etched substrate was then cleaned with saturated KOH solution in ethanol, acetone and ethanol. A compact TiO_2 gel was then applied to a substrate by spin-coating at 4 000 $r\cdot min^{-1}$ for 30 s, followed by annealing at 550 ℃ for 1 h in air. A mesoporous TiO_2 layer (1:3 with ethanol) by weight was applied at 4 000 $r\cdot min^{-1}$ for 40 s. The glass/FTO/compact TiO_2/mesoporous TiO_2 substrates were preheated at 550 ℃ for 30 min prior to spin-casting $FAPbI_3$, thin $FAPbI_3$ perovskite layer was formed by spin-coating of 30wt% Pb(OH)I:FAI mixture in *N*,*N*-Dimethylformamide (DMF) at 4 000 $r\cdot min^{-1}$ for 30 s in a argon-filled glove box, the molar ratio of Pb(OH)I to FAI was 1∶3. The color of the film gradually darkened after annealing on a heating hotplate for 30 min. Then, 10 $mg\cdot mL^{-1}$ P3HT (Poly (3-hexylthth iophene-2,5-diyl) regioregular, electronic grade, 99.995% trace metals basis, average M_r 30 000~60 000) (Sigma-Aldrich, St. Louis, MO, USA) in 1,2-dichlorobenzene was spin coated on the surface of $FAPbI_3$ perovskite film at 2 000 $r\cdot min^{-1}$ for 30 s to serve as the hole transport layer[15]. Finally, 100 nm Au were thermally evaporated on the substrate inside a vacuum chamber (5×10^5 Pa). The active area of the device is 0.09 cm^2. *J-V* characteristics were measured (2400 Series Source Meter, Keithley Instruments) under simulated AM 1.5G sunlight at 100 $mW\cdot cm^{-2}$.

1.5 Characterization

X-ray diffraction (XRD) patterns from the powder and perovskite films were obtained using a microdiffractometer (D8-Advance, Bruker, Karlsruhe, Germany)(Cu $K\alpha$, λ=0.154 18 nm) in the range of 10°~80° at a scan rate(2θ) of 0.2°·s^{-1} under the operation conditions of 30 kV and 40 mA, respectively. Scanning electron microscopy (SEM, S-4800, Hitachi, Japan) was used to investigate the cross-sectional structure and the surface morphology of the $FAPbI_3$ film on a 10 kV. The optical absorbance spectra of glass/$FAPbI_3$ perovskite film were measured using a UV-Vis-NIR spectrophotometer (U-4100, Hitachi, Japan) in the range of 200~900 nm at a scan speed of 300 $nm\cdot min^{-1}$ and sampling interval of 0.5 nm. The device characteristics and *J-V* responses of the solar cells, were measured using an analyzer (2400 Series Sourcemeter, Keithley, Cleveland, OH) under simulated AM 1.5G one sun 100 $mW\cdot cm^{-2}$ irradiation (Oriel Sol3A Class AAA Solar Simulator, Newport Corp., Irvine, CA, USA). The active area of the solar cells was 0.09 cm^2, which is defined by the overlapping area of the FTO and Au.

2 Results and discussion

2.1 X-Ray Diffraction of Pb(OH)I

X-ray diffraction pattern of the as-synthesized Pb(OH)I powder is shown in Fig.1. All of the diffraction peaks are indexed according to the orthorhombic Pb(OH)I structure with the PDF number of 22-0655 standard peaks of (101), (002), (102), (201), (111), (103), (202), (112), (210), (211), (010), (203), (001), (104), (302), which is also in good agreement with the reported XRD pattern[14]. The sharp

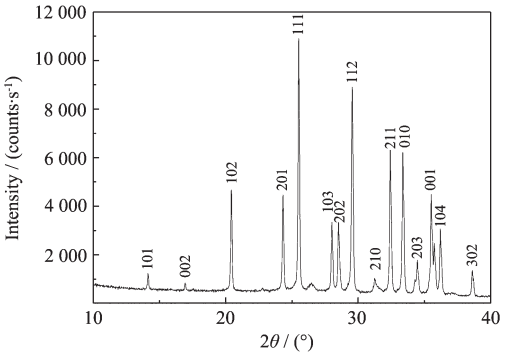

Fig.1 X-ray diffraction pattern of the as-synthesized Pb(OH)I powder

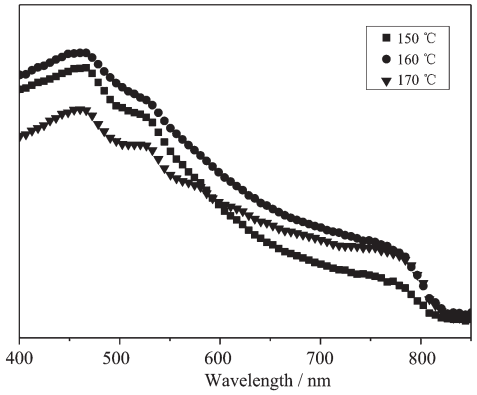

Fig.2 UV-Vis spectra for $FAPbI_3$ films annealed at different temperatures

diffraction peaks further indicate its high crystallinity fabricated by the solution reaction (**1**).

2.2 UV-Vis Absorption

The UV-Vis absorption spectra of the perovskite material deposited on FTO glasses and annealed at different temperatures are presented in Fig.2. All the samples exhibit an absorption onset at ~825 nm, which is very close to $FAPbI_3$ formed by a two-step method[6] and $FAPbI_{3-x}Cl_x$ formed by $PbCl_2$ based method. The sample annealed at 150 ℃ shows a low absorbance due to an uncompleted transformation of the $FAPbI_3$ perovskite. Increasing the annealing temperature to 160 ℃ leads an obvious increase in absorbance from 400 nm to 825 nm as shown in Fig.2. Further increasing the annealing temperature (170 ℃) results in a decrease of the absorption especially for the low wavelength light, which possibly due to shrinking and/or the decomposition of the $FAPbI_3$ perovskite film.

2.3 X-Ray diffraction of $FAPbI_3$

The XRD patterns of the perovskite films annealed at 150, 160 and 170 ℃ are presented in Fig. 3A. As expected, low annealing temperature results in incomplete conversion to *P*3*m*1 $FAPbI_3$ perovskite. The low annealing temperature leads not only to a decrease in diffraction intensity but also the appearance of an yellow $P6_3mc$ $FAPbI_3$ phase (#). As the annealing temperature is increased to 160 ℃ as shown in Fig.3b, which shows seven sharp reflections peaks at the following 2θ values: 13.8°, 19.6°, 24.9°, 27.9°, 31.4°, 39.9°, 42.5°, corresponding to the ($\bar{1}$11), (012), (003), ($\bar{2}$22), ($\bar{1}$23), (024), (015) reflections of pure *P*3*m*1 $FAPbI_3$ as reported [12], the intensity of the

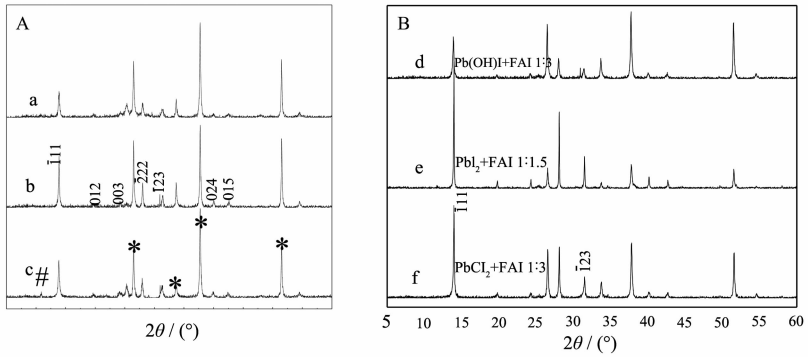

A: (a)150 ℃; (b)160 ℃; (c)170 ℃ B: (d) $n_{Pb(OH)I}/n_{FAI}$=1:3 160 ℃; (e) n_{PbI_2}/n_{FAI}=1:1.5 140 ℃; (f) n_{PbCl_2}/n_{FAI}=1:3 140 ℃.

Fig.3 XRD patterns of perovskite samples annealed at different temperatures (A). The perovskite was deposited on mesoporous TiO_2 coated onto FTO substrates. The figure indicates that the peaks associated with a new yellow $P6_3mc$ $FAPbI_3$ phase (#) and the FTO/mTiO_2 substrate (*). Comparison of XRD patterns of the pure $FAPbI_3$ and Cl-doped $FAPbI_3$ thin films (B)

perovskite ($\bar{1}11$), ($\bar{2}22$), and ($\bar{1}\bar{2}3$) peaks increases compared to the sample annealed at 150 ℃, which is attributed to the increased conversion rate. For the sample heated at 170 ℃, the decreased peak intensity of the perovskite is associated with the decomposition of perovskite phase. Additionally, the XRD patterns of the solution processed $FAPbI_3$ (or $FAPbI_{3-x}Cl_x$) film on the porous TiO_2 films from different lead precursors are also compared in Fig. 3B. The intensity ratio of the diffraction peak ($\bar{1}11$) to ($\bar{1}\bar{2}3$) could be employed to evaluate the orientation of the perovskite films. The PbI_2 derived $FAPbI_3$ perovskite film has the highest ($\bar{1}\bar{2}3$)/($\bar{1}11$) intensity ratio indicating its weak textured structure. The $PbCl_2$ derived $FAPbI_3Cl_{3-x}$ perovskite film has the lowest ($\bar{1}\bar{2}3$)/($\bar{1}11$) intensity ratio, which is attributed to its preferred orientation character. With Pb(OH)I as the lead precursor, the ($\bar{1}\bar{2}3$)/($\bar{1}11$) intensity ratio is obviously lower than that of PbI_2 derived $FAPbI_3$ perovskite film, but close to that of the $PbCl_2$ derived $FAPbI_3Cl_{3-x}$ film. The textured structure is critical for the transport of hole and electrons in the perovskite film without recombination. The method presented in this paper is a very efficient one-step solution processing approach for the fabrication of the textured triiodide perovskite film.

2.4 SEM

SEM images of perovskite films prepared at different annealing temperatures. These SEM images are shown in Fig.4. The perovskite films possess different morphologies on the mesoporous TiO_2 substrates with the domain size of capping domains up to micro-scale. In Lü′s work[13], there was an obvious shrinkage of the $FAPbI_{3-x}Cl_x$ perovskite capping layer was related to the decomposition of the perovskite phase, the coverage of the perovskite capping layer is only about 50% when the annealing temperature is 140 ℃. In this work, as annealing temperature increases from 150 ℃ to 170 ℃ (Fig.4a, 4b. 4c), the domain size increases, leading to a reduction of the surface coverage of the capping layer, the coverage of the perovskite capping layer is still over 90% at 160 ℃. It indicates that the Pb(OH)I derived $FAPbI_3$ film delivers a higher morphological stability than the traditional $FAPbI_{3-x}Cl_x$. As shown in the magnified SEM image of the perovskite film annealed at 150 ℃ (Fig.4d), the capping domains appear a textured structure compacted with several single perovskite particles. Along with the increase of the annealing temperature to 160 ℃ as shown in Fig.4e, the textured structure and the boundary of the perovskite particles

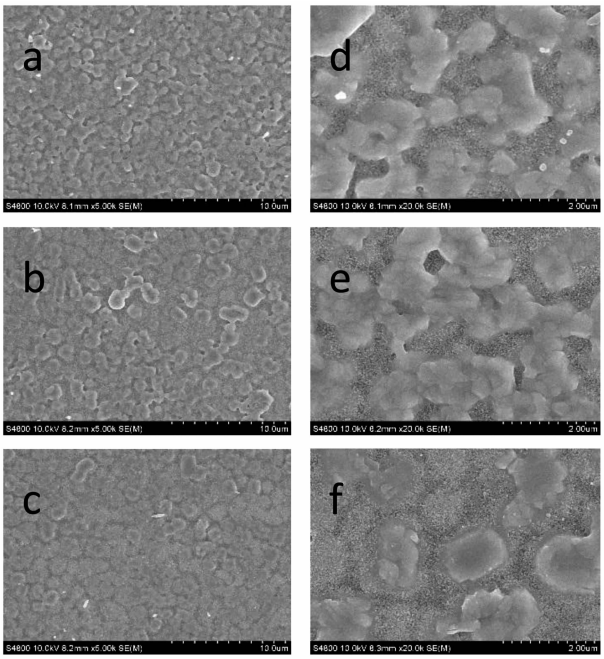

Fig.4　SEM images of TiO_2 films with deposited perovskite solution heat treated at (a~d) 150 ℃, (b~e) 160 ℃, (c~f) 170 ℃

become more obviously. Further increase the annealing temperature to 170 ℃, the textured perovskite domains start to shrink and decompose, leaving a more smooth surface (Fig.4f).

2.5 Photovoltaic Performance

Fig.5 shows a cross-sectional SEM image of the device assembled in this study (a). There are six layers, such as glass, FTO, compact TiO_2 layer (~50 nm), mesoporous TiO_2 layer and $FAPbI_3$ perovskite (~400 nm), P3HT hole transporting layer (HTL, ~100 nm), and Au electrode (~100 nm)(b).

J-V curves show that the annealing temperature at 160 ℃ demonstrates higher J_{SC} which is probably due to formation of pure *P*3*m*1 perovskite and better conversion efficiency than devices annealing at 150 ℃ and 170 ℃, as low annealing temperature at 150 ℃ results in incomplete conversion to *P*3*m*1 $FAPbI_3$ perovskite and perovskite start to shrink and decompose at 170 ℃. The best PCE was obtained due mainly to the highest short-circuit ~current (J_{SC}) and open-circuit voltage (V_{OC}) (J_{SC}=18.6 mA cm^{-2}, V_{OC}= 0.67 V, FF (Fill Factor)=46.9%, PCE=5.8% in Table 1).

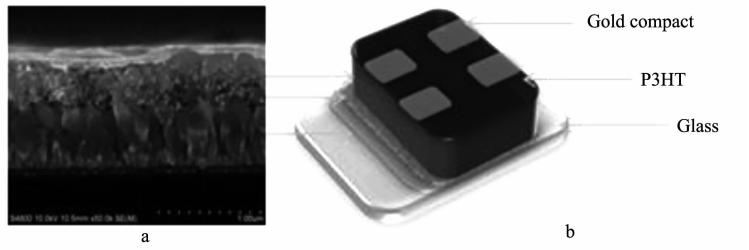

Fig.5 (a) Cross-sectional SEM image and (b) schematic illustration of the architecture for the perovskite devices fabricated in this work

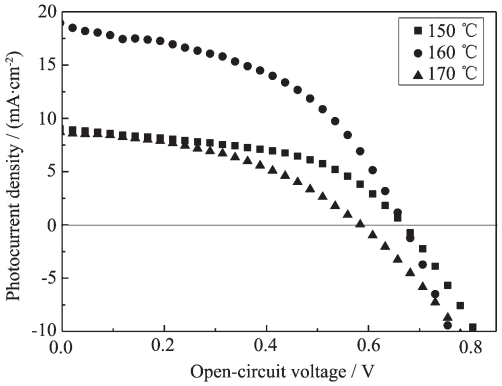

Fig.6 *J-V* characteristics taken under standard AM1.5G illumination (100 mW·cm^2) and devices made using different annealing temperatures for the perovskite

From *J-V* curves of the perovskite devices, the average PCE of perovskite solar cells reaches about 6%. However, compared with the V_{OC} and J_{SC} both of $FAPbI_3$ (or $FAPbI_{3-x}Cl_x$) film from different lead precursors, the Pb(OH)I derived $FAPbI_3$ film delivers higher V_{OC} and J_{SC} than that of the PbI_2 derived $FAPbI_3$ film but lower than the values of traditional $FAPbI_{3-x}Cl_x$. That is probably because that pure $FAPbI_3$ buy using Pb(OH)I as precursor is easier to obtain and a two-step method can obtain higher crystallinity films than one-step solution processing method[13,16]. And there are lots of traps on the surface of capping layer which is responsible for carrier recombination by using one-step spinning method[17], as a result the V_{OC} and J_{SC} are lower than the values of traditional $FAPbI_{3-x}Cl_x$. The slightly lower FF is largely attributed to the decrease of capping layer coverage and the parallel resistance of the devices in this pin-hole free

Table 1 Photovoltaic parameters of devices fabricated

Temperature / ℃	V_{OC} / mV	J_{SC} / (mA·cm^{-2})	Fill Factor / %	PCE / %
150	668	9.0	49.5	3.0
160	668	18.6	46.9	5.8
170	584	8.6	43.1	2.2

V_{OC}: open-circuit voltage, J_{SC}: photocurrent density, PCE: photoelectric conversion efficiency

thin film [18] and the selective contacts formed by TiO_2 and P3HT are not yet optimized for minimal resistance and, therefore, present another source of loss in fill factor[19].

3 Conclusions

We have applied Pb(OH)I to synthesize the pure phase $FAPbI_3$ perovskite and fabricate corresponding mesoscopic solar cells. The results indicate that annealing temperature has an important effect on crystallinity, the morphology of capping layer and performance of photovoltaic system etc, and a pure perovskite can be obtained at 160 ℃ annealing which leads to higher J_{SC}(18.6 mA·cm^{-2}) and PCE(5.8%) than 150 ℃ and 170 ℃. Pb(OH)I is a kind of high crystallinity and low cost compound, employing Pb(OH)I to substitute PbI_2 and $PbCl_2$ to synthesize the pure $FAPbI_3$ which shows good performance of photovoltaic cells, excellent thermal stability and high capping layer coverage. Although the current efficiency of the solution based $FAPbI_3$ perovskite solar cells is still lower than that of prepared from the traditional PbI_2 and $PbCl_2$ based method, further efforts in optimization of the processing will lead to a comparable or higher efficiency through better control over all the processing parameters by using various methods, such as one-step method with additive and anti-solvent engineering[20] or optimizing devices structure etc, to decrease the traps on capping layer.

References:

[1] Chen H W, Pan X, Liu W Q, et al. *Chem. Commun*., **2013**, **49**:7277-7279

[2] Stranks S D, Eperon G E, Grancini G, et al. *Science*, **2013**, **342**(6156):341-344

[3] Park N G. *J. Phys. Chem. Lett*., **2013**,**4**(15):2423-2429

[4] Qiu J H, Qiu Y C, Yan K Y, et al. *Nanoscale*, **2013**,**5**(8): 3245-3248

[5] Rhee J H, Chung C C, Diau EW-G, et al. *NPG Asia Mater*., **2013**,**5**(10):e68 (DOI:10.1038/am.2013.53)

[6] Lee J W, Seol D J, Cho A N, et al. *Adv. Mater*., **2014**,**26** (29):4991-4998

[7] Jeon N J, Lee J, Noh J H, et al. *J. Am. Chem. Soc*., **2013**,**135**(51):19087-19090

[8] Krishnamoorthy T, Kunwu F, Boix P P, et al. *J. Phys. Chem. A*, **2014**,**2**(18):6305-6309

[9] Hodes G, Cahen D. *Nat. Photon*., **2014**,**8**(2):87-88

[10]Koh Teck Ming, Fu Kunwu, Fang Yanan, et al. *J. Phys. Chem. C*, **2014**,**118**(30):16458-16462

[11]Eperon G E, Stranks S D, Menelaou C, et al. *Energy Environ. Sci*., **2014**,**7**(3):982-988

[12]Pang S P, Hu H, Zhang J, et al. *Chem. Mater*., **2014**,**26**(3): 1485-1491

[13]Lü S L, Pang S P, Zhou Y Y, et al. *Phys. Chem. Chem. Phys*., **2014**,**16**(36):19206-19211

[14]Zhu G Q, Liu P, Hojamberdiev M, et al. *Appl. Phys. A*., **2009**,**98**(2):299-304

[15]WANG Dong(王栋), ZHU Hui-Min(朱慧敏), ZHOU Zhong-Min(周忠敏), et al. *Acta Phys. Sin.* (物理学报), **2015**,**3**(64): 38403-38411

[16]Pellet N, Gao P, Gregori G, et al. *Angew. Chem. Int. Ed.*, **2014**,**53**(12):3151-3157

[17]YANG Zhi-Sheng(杨志胜), YANG Li-Gong(杨立功), WU Gang(吴刚), et al. *Acta Chim. Sin.*(化学学报), **2011**,**6** (69):627-632

[18]Chen Q, Zhou H P, Hong Z R, et al. *J. Am. Chem. Soc*., **2014**,**136**(2):622-625

[19]Conings B, Baeten L, De Dobbelaere C, et al. *Adv. Mater*., **2014**,**26**(13):2041-2046

[20]Zhao Y X, Zhu K. *J. Phys. Chem. Lett*., **2014**,**23**(5):4175-4186